Detecting discrete spacetime via matter interferometry

Todd A. Brun[*] and Leonard Mlodinow[†]

Center for Quantum Information Science and Technology, University of Southern California, Los Angeles, California 90089, USA

(Received 6 April 2018; published 7 January 2019)

If the structure of spacetime is discrete, then Lorentz symmetry should only be an approximation, valid at long length scales. At finite lattice spacings there will be small corrections to the Dirac evolution. In particular, the lattice structure will be reflected in a modification of the free-particle dispersion relation. We show that these can produce a surprisingly large phase shift between the two arms of a nonparallel interferometer. This method could be employed to test any model that predicts a direction-dependent dispersion relation. Here, we calculate the size of this phase shift for a particular model, the three-dimensional quantum walk on the body-centered cubic lattice, which has been shown to give rise to the Dirac equation in the continuum limit. Though the details of this model will affect the size of the shift, its magnitude is set largely by dimensional analysis, so there is reason to believe that other models would yield similar results. We find that, with current technology, a modest-sized neutron interferometer could detect lattice spacings as small as 10^{-31} m, 13 orders of magnitude smaller than the scale probed by the LHC. A suitably scaled-up experiment could possibly detect lattice spacings even at the Planck scale.

DOI: 10.1103/PhysRevD.99.015012

I. INTRODUCTION

A. Discrete spacetime and Lorentz violation

Lorentz symmetry, which underlies special and general relativity, has been tested to remarkable precision, and so far has passed every test. This has not, however, prevented speculation that Lorentz symmetry might be violated at very high energies and very short length scales. Over the years, a number of theories have been proposed that would lead to Lorentz violation, and a number of experiments have been suggested to test for such violations.

Dirac proposed that Lorentz invariance violation might play a role in physics in the 1950s [1], followed by several others in the years that followed (e.g., Refs. [2–4]). In the 1990s, influential papers by Coleman and Glashow raised the subject of systematic tests of Lorentz violation within the context of elementary particle physics [5,6]. Various theories of quantum gravity have also suggested that Lorentz invariance may not be an exact symmetry [7–10]. In those theories, the natural scale at which one would expect to observe that violation is at the Planck energy of approximately 10^{19} GeV, which would correspond to a distance scale of the Planck length, $M_{\mathrm{Pl}} = 1.616 \times 10^{-35}$ m. One type of Lorentz noninvariance that has been considered arises from discrete spacetime. Some suggest that, at scales smaller than M_{Pl}, the usual notions of space and distance may not even make sense [11].

The Planck energy is not just far higher than current accelerator energies of approximately 10^3 GeV, but also far higher than the energy of the most energetic observed particles: the ultra high-energy cosmic rays with energies as high as 10^{11} GeV $\approx 10^{-8} M_{\mathrm{Pl}}$. However, large violations of Lorentz invariance at the Planck scale can lead to a small degree of violation at much lower energies, presenting the possibility of detection at more realistic scales. For example, Lorentz violation could imply that neutrino oscillation will occur even if the neutrino mass is zero [12]. Lorentz violation can also shift the threshold for elementary particle reactions, or lead to the occurrence of processes such as photon decay and the vacuum Cherenkov effect that would be forbidden in a Lorentz-invariant theory. As a result, the past few decades have seen a growing literature on tests of Lorentz invariance, and on the placement of bounds on a variety of proposed deviations (for recent reviews, see Refs. [13,14]).

One would expect the nature of proposed Lorentz violations to depend upon the specifics of the Lorentz-violating theory, but one common implication of such theories is an alteration of a particle's dispersion relation, which relates the particle's energy to its momentum and mass [13,14]. If spacetime has a discrete structure—such as an underlying lattice—these effects should be nonisotropic, giving different shifts in different directions. A family of models that lead to such Lorentz violation are quantum walks and quantum cellular automata.

Different Lorentz-violating effects have been broadly categorized within the Standard Model Extension (SME)

[*]tbrun@usc.edu
[†]lmlodinow@gmail.com

framework [15–21]. For a free fermion these effects show up as additional terms in the Dirac equation. The strengths of these possible terms are quantified by several families of parameters. There are stringent experimental limits on the size of most of these parameters, based on many different types of experiments. We show below how the corrections to the Dirac equation arising from the three-dimensional (3D) quantum walk fit into the SME framework, and how the experimental sensitivity we project in this paper for a matter interferometer may compare to other experimental limits.

B. Quantum walks

Quantum walks—unitary analogues of classical random walks—were proposed both as possible constructions for quantum algorithms, and for simple models of quantum systems worthy of study for their own sake [22–27]. In a discrete-time quantum walk (the focus of the current work), a particle moves on a graph, with the vertices representing possible particle positions and the edges the connections between them. In addition to its position, such a particle has an internal space (often called the "coin space") which allows for nontrivial dynamics.

A body of work has shown that quantum walks on regular lattices in 1D, 2D and 3D can have as their continuum limit a relativistic quantum equation such as the Weyl and Dirac equations [28–45]. In a previous work [46], we have shown that a particular construction of a 3D quantum walk on the body-centered cubic (BCC) lattice gives rise to the Dirac equation in that limit if it is invariant under parity transformations and discrete rotations of the coordinate axes.

According to that model, if spacetime were discrete the Dirac equation would be only approximately correct, and the degree to which nature deviates from the Dirac theory, and whether those deviations are observable, would be determined by the size of the lattice spacing Δx. Experimental tests and astrophysical observations can therefore place upper limits on Δx.

The most glaring difference between the discrete and continuum theories is that Lorentz invariance is violated in the discrete theory [47,48]. In particular, the dispersion relation predicted by the quantum walk theory differs from that of the Dirac theory, in that the square of the energy, which is $m^2c^4 + p^2c^2$ for the Dirac theory, includes additional terms of order $k\Delta x$ and higher, which vanish in the continuum limit. These higher-order terms can be seen as corrections to the continuum limit, which would act as perturbations to the usual Dirac evolution.

These terms have a directional dependence that could make them detectable in a suitably designed (nonparallel) matter interferometer. In this paper, we analyze the phase shift of such a matter interferometer, and calculate the magnitude of the shift for thermal neutrons. The result, as we will see, is surprisingly large. With interferometer sizes and accuracies typical of current neutron interferometers, one could put very stringent limits on the size of the lattice spacing. Scaling up in accuracy by roughly 3 orders of magnitude would allow one to test for discreteness at the Planck scale.

While the current calculations are specific to our particular 3D quantum walk model, such an experiment should also be able to see the effects of other theories with direction-dependent corrections to Lorentz invariance. An experiment of this type would therefore test a whole family of Lorentz-violating models.

C. This paper

In Sec. II of this paper we describe the 3D quantum walk on the BCC lattice, and derive its momentum-space representation. In Sec. III, we expand the evolution operator in the long-wavelength limit, and equate that to the perturbation expansion of a Hamiltonian operator, which is the Dirac Hamiltonian to leading order, but has direction-dependent corrections at the next order. This perturbation would produce spin- and direction-dependent energy shifts, which are calculated in Sec. IV. These shifts would in turn lead to phase shifts in an interferometer.

In Sec. V A we calculate the size of the relative phase shifts between the two arms of a nonparallel Mach-Zehnder interferometer. This decomposes into the product of a quantity $(pmcL\Delta x/\hbar^2)$ that depends on the particle mass m, its momentum p, the linear size of the interferometer L and the lattice spacing Δx, and a geometrical factor that depends on the layout of the interferometer and its orientation with respect to the underlying spatial lattice. Though we calculate these quantities for our particular quantum walk model, the magnitude of the corrections is set largely by dimensional analysis, so one could reasonably expect that the size of the phase shifts predicted by other models would be comparable. In Sec. V B we calculate the size of these phase shifts for a neutron interferometer with thermal neutrons, and estimate the limits that could be put on Δx by current experimental abilities. In Sec. V C we compare our results to the SME framework, and show that our corrections can be identified with two sets of parameters in that framework. We briefly consider existing experimental limits (or lack thereof) on these parameters, and how limits on these parameters would imply limits for Δx. Finally, in Sec. VI we discuss our results.

II. 3D QUANTUM WALK

The unitary operator giving one step of the 3D quantum walk on the body-centered cubic lattice is

$$U = (S_X P_X^+ + S_X^\dagger P_X^-)(S_Y P_Y^+ + S_Y^\dagger P_Y^-) \times (S_Z P_Z^+ + S_Z^\dagger P_Z^-) e^{-i\theta Q}, \quad (1)$$

where $P^{\pm}_{X,Y,Z}$ are projectors onto the internal "coin" space, indicating whether the particle should step in the positive or negative direction along the X, Y, or Z axis, and $S_{X,Y,Z}$ shifts the particle by one lattice position along the X, Y or Z axis. This unitary operator U has the form of three successive 1D quantum walks on the line, sharing the same internal space. The operator Q is the "coin flip" operator, which applies a rotation to the internal space.

We can most readily go to the continuum limit by transforming to the momentum representation:

$$|k_x, k_y, k_z\rangle = \sum_{\ell,m,n=-\infty}^{\infty} e^{-i(k_x \ell \Delta x + k_y m \Delta x + k_z n \Delta x)} |\ell \Delta x, m\Delta x, n\Delta x\rangle, \qquad -\pi < k_{x,y,z}\Delta x \le \pi. \tag{2}$$

These are eigenstates of the shift operators $S_{x,y,z}$ with eigenvalues $e^{ik_{x,y,z}\Delta x}$. In terms of this basis, the unitary evolution operator becomes

$$U = \int\int\int d^3\mathbf{k}\, e^{ik_x \Delta x \Delta P_X} e^{ik_y \Delta x \Delta P_Y} e^{ik_z \Delta x \Delta P_Z} e^{-i\theta Q} \otimes |k_x, k_y, k_z\rangle\langle k_x, k_y, k_z|, \tag{3}$$

where $\Delta P_{X,Y,Z} \equiv P^{+}_{X,Y,Z} - P^{-}_{X,Y,Z}$, and Δx is the lattice spacing. As shown in earlier work [46] these three $\Delta P_{X,Y,Z}$ operators and the coin flip operator Q must all mutually anticommute. Up to a unitary equivalence, these must therefore be the same as the operators in the Weyl representation of the Dirac equation:

$$\begin{aligned} \Delta P_X &= \gamma_0\gamma_1 = -\sigma_Z \otimes \sigma_X, \\ \Delta P_Y &= \gamma_0\gamma_2 = -\sigma_Z \otimes \sigma_Y, \\ \Delta P_Z &= \gamma_0\gamma_3 = -\sigma_Z \otimes \sigma_Z, \\ Q &= \gamma_0 = -\sigma_X \otimes I. \end{aligned} \tag{4}$$

We assume that one step of the quantum walk represents a time Δt, and define a limiting velocity $\Delta x/\Delta t \equiv c$. The continuum limit is the limit where the wavelength is very long compared to the lattice spacing, which is $|k\Delta x| \ll 1$ for $k = \sqrt{k_x^2 + k_y^2 + k_z^2}$. We also need the coin flip parameter θ to be small, so that in a single infinitesimal time step the coin flip operation is also infinitesimal. Given a fixed finite Δx, the parameter θ is fixed by the particle mass: $\theta \equiv mc\Delta x/\hbar$.

Note that it has been shown that quantum walks of the standard form only lead to the 3D Dirac equation in the long-wavelength limit on the body-centered cubic lattice [28]. This does not quite rule out other theories on discrete spacetime with a different mathematical form, though we do not know any examples of such theories. However, we suspect that any such theory would have a perturbative expansion that is at least qualitatively similar to the one we find below.

III. PERTURBATION EXPANSION

As we approach the continuum limit, we can expand the unitary evolution operator in powers of $k\Delta x$. The leading-order (linear) term produces the Dirac equation. But there are corrections to this evolution at quadratic and higher orders. How can we consistently capture the effects of these corrections?

Our approach is to identify the time evolution operator with a Hamiltonian evolution, and then expand this Hamiltonian in a perturbation expansion. That is, we equate

$$\begin{aligned} U = \int\int\int d^3\mathbf{k}\, e^{-i(\Delta t/\hbar)(H_0(\mathbf{k}) + H_1(\mathbf{k}) + \cdots)} \\ \otimes |k_x, k_y, k_z\rangle\langle k_x, k_y, k_z|, \end{aligned} \tag{5}$$

where the H_i operators act on the internal space, $H_0(\mathbf{k})$ is zeroth order in $k\Delta x$, $H_1(\mathbf{k})$ is first order, and so forth. With U given by Eq. (3), we can expand both sides of Eq. (5) and equate them order by order. At leading order we get the Dirac Hamiltonian:

$$H_0(\mathbf{k}) = -mc^2 Q + c\hbar(k_x \Delta P_X + k_y \Delta P_Y + k_z \Delta P_Z). \tag{6}$$

Making the operator choices described by Eq. (4), and the usual identification of $\hbar\mathbf{k} = \mathbf{p}$, we get

$$H_0(\mathbf{k}) = -mc^2 \sigma_X \otimes I + c\sigma_Z \otimes (p_x \sigma_X + p_y \sigma_Y + p_z \sigma_Z). \tag{7}$$

The eigenvalues of $H_0(\mathbf{k})$ are $\pm\sqrt{m^2c^4 + c^2p^2} \equiv \pm E_0$, where $p^2 = p_x^2 + p_y^2 + p_z^2$, and both eigenvalues are doubly degenerate.

At the next order in the expansion we get the equation

$$\begin{aligned} (1/2)(\Delta t/\hbar)^2 H_0^2(\mathbf{k}) + (i\Delta t/\hbar) H_1(\mathbf{k}) \\ = (1/2)(k^2 + \theta^2) I + k_x k_y \Delta P_X \Delta P_Y \\ + k_x k_z \Delta P_X \Delta P_Z + k_y k_z \Delta P_Y \Delta P_Z \\ + \theta(k_x \Delta P_X + k_y \Delta P_y + k_z \Delta P_z) Q. \end{aligned} \tag{8}$$

Inserting our above expression for $H_0(\mathbf{k})$ and solving for $H_1(\mathbf{k})$, we get

$$H_1(\mathbf{k}) = \frac{c\Delta x}{\hbar}[I \otimes (-p_y p_z \sigma_X + p_x p_z \sigma_Y - p_x p_y \sigma_Z) - mc\sigma_Y \otimes (p_x\sigma_X + p_y\sigma_Y + p_z\sigma_Z)]. \quad (9)$$

We could in principle continue the expansion to find higher orders of the perturbation series, but this first-order correction is already sufficient to produce observable consequences. In particular, it produces energy shifts for free particles of equal momentum in different directions relative to the lattice.

IV. ENERGY SHIFTS

For a positive-energy eigenstate $|v\rangle$ of Hamiltonian $H_0(\mathbf{k})$ with energy $E_0 = \sqrt{m^2c^4 + p^2c^2}$, the next term in the perturbation expansion will produce a shift in energy

$$\Delta E_v(\mathbf{k}) = \langle v|H_1(\mathbf{k})|v\rangle. \quad (10)$$

We can find the eigenvectors of $H_0(\mathbf{k})$ and calculate this energy shift exactly. Let us rewrite this Hamiltonian as follows:

$$\begin{aligned} H_0(\mathbf{k}) &= -mc^2\sigma_X \otimes I + c\sigma_Z \otimes (p_x\sigma_X + p_y\sigma_Y + p_z\sigma_Z) \\ &= -mc^2\sigma_X \otimes I \\ &\quad + pc\sigma_Z \otimes \left(\frac{p_x}{p}\sigma_X + \frac{p_y}{p}\sigma_Y + \frac{p_z}{p}\sigma_Z\right) \\ &\equiv -mc^2\sigma_X \otimes I + pc\sigma_Z \otimes \Phi_{\hat{\mathbf{p}}}, \end{aligned} \quad (11)$$

where

$$\Phi_{\hat{\mathbf{p}}} = \left(\frac{p_x}{p}\sigma_X + \frac{p_y}{p}\sigma_Y + \frac{p_z}{p}\sigma_Z\right). \quad (12)$$

The operator $\Phi_{\hat{\mathbf{p}}}$ depends on the direction $\hat{\mathbf{p}} = \mathbf{p}/p$, and has eigenvalues ± 1. Let us define its corresponding eigenvectors to be $|\phi_\pm\rangle$. Then we can rewrite $H_0(\mathbf{k})$ as

$$\begin{aligned} H_0(\mathbf{k}) &= (-mc^2\sigma_X + pc\sigma_Z) \otimes |\phi_+\rangle\langle\phi_+| \\ &\quad + (-mc^2\sigma_X - pc\sigma_Z) \otimes |\phi_-\rangle\langle\phi_-| \\ &= E_0\left[\left(-\frac{mc^2}{E_0}\sigma_X + \frac{pc}{E_0}\sigma_Z\right) \otimes |\phi_+\rangle\langle\phi_+| \right. \\ &\quad \left. + \left(-\frac{mc^2}{E_0}\sigma_X - \frac{pc}{E_0}\sigma_Z\right) \otimes |\phi_-\rangle\langle\phi_-|\right], \\ &\equiv E_0\left[\Psi_+ \otimes |\phi_+\rangle\langle\phi_+| + \Psi_- \otimes |\phi_-\rangle\langle\phi_-|\right], \end{aligned} \quad (13)$$

where the operators $\Psi_\pm$ are

$$\Psi_\pm = \left(-\frac{mc^2}{E_0}\sigma_X \pm \frac{pc}{E_0}\sigma_Z\right) \quad (14)$$

and both have eigenvalues ± 1. Call the corresponding eigenvectors $|\psi_{\pm\pm}\rangle$. We can then identify two eigenvectors of $H_0(\mathbf{k})$ with positive energy E_0,

$$|v_1\rangle = |\psi_{++}\rangle \otimes |\phi_+\rangle, \qquad |v_2\rangle = |\psi_{-+}\rangle \otimes |\phi_-\rangle, \quad (15)$$

and two eigenvectors with negative energy $-E_0$,

$$|v_3\rangle = |\psi_{+-}\rangle \otimes |\phi_+\rangle, \qquad |v_4\rangle = |\psi_{--}\rangle \otimes |\phi_-\rangle. \quad (16)$$

Restricting ourselves to the positive-energy eigenspace, we can then calculate the energy shift due to the first-order perturbation Hamiltonian $H_1(\mathbf{k})$:

$$\begin{aligned} \langle v_2|H_1(\mathbf{k})|v_2\rangle &= \left(\frac{c\Delta x}{\hbar}\right)\frac{p_x p_y p_z}{2p} = -\langle v_1|H_1(\mathbf{k})|v_1\rangle, \\ \langle v_1|H_1(\mathbf{k})|v_2\rangle &= \left(\frac{c\Delta x}{\hbar}\right)\sqrt{\left(\frac{m^2c^2}{m^2c^2+p^2}\right)\left(\frac{p^2-p_z^2}{p^2}\right)} \\ &\quad \times (p_x p_y - ipp_z) = \langle v_2|H_1(\mathbf{k})|v_1\rangle^*. \end{aligned} \quad (17)$$

We see that the energy shift produced by the perturbation depends on the *internal state* (spin) of the particle, and its *direction*. These energy shifts should produce relative phase shifts between particles propagating in different directions. This suggests in turn that a suitably arranged interferometer could, in principle, detect the effect of spacetime discreteness.

V. INTERFEROMETER

Ever since the classic Michelson-Morley experiment [49], interferometry has been a powerful tool to search for direction dependence or other Lorentz violations in physics. More recently, there have been experiments probing for new physics, e.g., with electron orbitals in trapped ions [50] and with photons [51]. In the section below, we calculate the phase shifts produced by the next-order corrections to the Dirac Hamiltonian in an interferometer, and estimate the performance of a neutron interferometer in detecting the discreteness of spacetime.

A. Interferometer layouts

To analyze the effect on an interferometer, we will treat the spatial degrees of freedom of the particle semiclassically, but the internal state of the particle quantum mechanically. That is, we will assume that the particle is propagating in a wave packet that is broad enough in space to have a very narrow spread in momentum space about some central momentum $\mathbf{p}$, so that we can treat $\mathbf{p}$ as a

definite value in solving for the evolution of the internal state. So long as the uncertainty in momentum is very small compared to the momentum itself, the effect on the phase shift should be negligible.

Consider a wave packet with central momentum $\mathbf{p}$ propagating in a straight line over a distance L. The time to traverse that distance is

$$t = \frac{L}{c}\sqrt{\frac{m^2c^2 + p^2}{p^2}}. \tag{18}$$

The state should accumulate a phase of

$$\phi = -\frac{\langle H_1(\mathbf{k})\rangle t}{\hbar}.$$

If the internal state of the particle is prepared in the eigenstate $(|v_1\rangle + |v_2\rangle)/\sqrt{2}$ of the leading-order Hamiltonian $H_0(\mathbf{k})$, then this phase becomes

$$\begin{aligned}\phi &= \left(\frac{L\Delta x}{\hbar^2}\right)\left(\frac{p_x p_y}{p}\right)\sqrt{\frac{m^2c^2(p_x^2 + p_y^2)}{p^2}} \\ &= g(\hat{\mathbf{p}})\left(\frac{pmcL\Delta x}{\hbar^2}\right),\end{aligned} \tag{19}$$

where the geometric factor

$$g(\hat{\mathbf{p}}) \equiv \frac{p_x p_y\sqrt{p_x^2 + p_y^2}}{p^3} \tag{20}$$

depends only on the direction $\hat{\mathbf{p}}$ of the momentum vector, and the rest of the expression in Eq. (19) depends only on its magnitude p.

We can now analyze the relative phase shift in an interferometer. Suppose that the interferometer has two arms; each arm is a sequence of straight line segments. The phase accumulated in one arm of the interferometer is the sum of the phases from each of the straight line segments, and the relative phase shift in the interferometer should then be the difference between the phases accumulated in each arm. Because the phase depends on the direction of momentum, a nonparallel interferometer could accumulate different phases in each arm; and the relative phase will also generally depend on the orientation of the whole interferometer with respect to the underlying spatial lattice.

Consider an interferometer with an arrangement like that shown in Fig. 1. The upper arm and lower arm are both of length L. Each arm consists of a diagonal segment of length $2L/3$ and a near-vertical segment of length $L/3$. Consider a 3D rotation $\mathbf{R}$. If we rotate all the segments of the interferometer by this 3D rotation, we can calculate their contributions to the phase shift in each of the arms. The relative phase shift between the upper and lower arms becomes

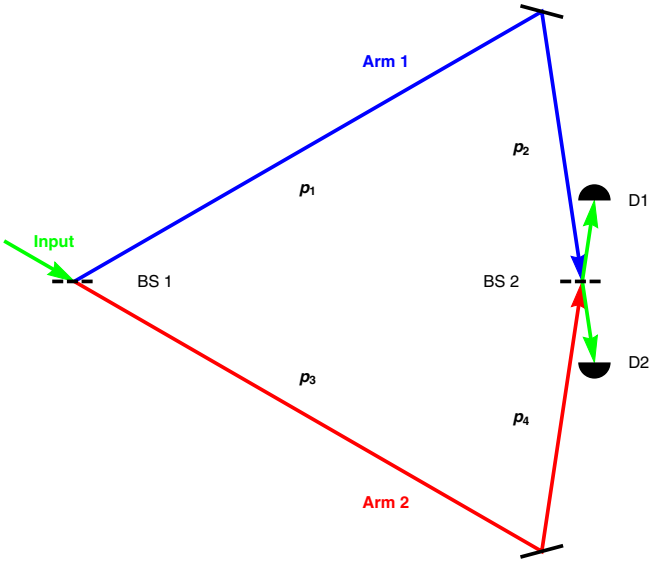

FIG. 1. A nonparallel Mach-Zehnder interferometer that exhibits a relative phase shift between the two arms, which is dependent on its orientation relative to the spatial lattice and the spin state of the particle. BS1 and BS2 are the beam splitters, and D1 and D2 are the detectors.

$$\Delta\phi \equiv \phi_1 - \phi_2 = G(\mathbf{R})\left(\frac{pmcL\Delta x}{\hbar^2}\right), \tag{21}$$

where $G(\mathbf{R})$ is an overall geometric factor depending on the arrangement of the interferometer and its orientation with respect to the underlying spatial lattice. For the interferometer depicted in Fig. 1, the factor $G(\mathbf{R})$ is

$$\begin{aligned}G(\mathbf{R}) = {}& (2/3)g(\mathbf{R}\hat{\mathbf{p}}_1) + (1/3)g(\mathbf{R}\hat{\mathbf{p}}_2) \\ & - (2/3)g(\mathbf{R}\hat{\mathbf{p}}_3) - (1/3)g(\mathbf{R}\hat{\mathbf{p}}_4),\end{aligned} \tag{22}$$

and ranges from roughly -0.57 to $+0.57$. In a random orientation $\mathbf{R}$ it typically takes values with magnitude of order 10^{-1}.

We have no reason to believe that the interferometer in Fig. 1 is optimal. We have found one nonplanar interferometer arrangement, e.g., which gives a geometrical factor that is even larger. The interferometer depicted here has the largest geometrical factor g of the small number of planar configurations we have analyzed, and large enough that it would not strongly suppress the signal in an experiment. Note, however, that a standard Mach-Zehnder interferometer configuration shaped like a parallelogram would have no signal: because there are parallel sides of equal length in each arm, the geometric factor is $g = 0$ for such an interferometer. That is why we have studied nonparallel configurations.

B. Neutron interferometry

Neutrons have many properties that are useful for such an interferometry experiment. They are uncharged fermions with high mass, so even thermal neutrons have relatively high momentum. They can be prepared in spin-polarized input beams with a narrow range of momenta. Physicists have a great deal of experience in designing and building high-precision neutron interferometers [52,53]. Let us consider a neutron interferometer with a configuration like that depicted in Fig. 1. The neutron has a mass $m = 1.675 \times 10^{-27}$ kg, and for thermal neutrons the momentum will be approximately $p = 3.7 \times 10^{-24}$ kg m/s. A typical neutron interferometer has an arm length of order $L = 10$ cm. Plugging these values into the formula in Eq. (21) and assuming a geometric factor of order $g \sim 10^{-1}$, we get a relative phase shift of order $3 \times 10^{24} \Delta x$ radians between the arms (where Δx is measured in meters). The phase shift is directly proportional to the lattice spacing Δx.

This phase shift is surprisingly large. We can see why this is so by looking back at the form of the perturbation in Eq. (17). We can understand these shifts as being our small, dimensionless expansion parameter $k\Delta x$ (where $k = p/\hbar$ is the wave number) multiplying terms with units of energy. These terms scale roughly as pc times a direction-dependent geometric factor. For a nonrelativistic particle (like a thermal neutron), this energy is small compared to the mass energy mc^2, but large compared to the nonrelativistic kinetic energy $p^2/2m$. An energy dependence like the former would certainly have been already ruled out by experiment; the latter would probably be undetectable in a nonrelativistic system. The quantum walk model, however, predicts a shift at an intermediate energy scale. (Note that there is no guarantee that other kinds of Lorentz-symmetry-violating theories would have the same scaling.)

A typical neutron interferometry experiment can resolve a phase shift on the order of 10^{-2} radians. This would be large enough to detect a lattice spacing Δx of about 3×10^{-27} m. To put that in perspective, the length scale probed at the LHC in CERN is about 10^{-18} m. The most accurate current neutron interferometers have a sensitivity as low as microradians [54,55], which could put bounds on lattice spacings of order 10^{-31} m.

If the lattice spacing is of the order of the Planck length, $\Delta x \sim 1.6 \times 10^{-35}$ m, that would require a phase sensitivity on the order of nanoradians. That is 3 or 4 orders of magnitude beyond the most accurate experiment to date. However, the difference is not so large that such a measurement is beyond conception: increasing the arm length to ~10 m and collecting data for a long period could conceivably close that gap.

In practice, one would probably need to detect the change in relative phase between the two arms in different orientations of the interferometer, to distinguish the effects of Lorentz violation from small errors in the arm lengths of the interferometer or other such systematic uncertainties. This raises some practical issues. Because the interferometer is tied to an incoming beam line from a nuclear reactor, it probably cannot be rotated into an arbitrary orientation. However, a small-scale interferometer (with arms of order 10 cm to 1 m) could be rotated azimuthally around the incoming beam line [54].

Of course, the interferometer is also on the surface of the Earth, which is rotating. Since the phase sensitivity is limited by shot noise, long data collection times might be needed to detect very small phase shifts. Assuming that the Earth's rotational axis has a fixed orientation relative to the underlying spatial lattice, one would expect the relative phase shift between the two arms to vary periodically with a period equal to the sidereal day (23 hours, 56 minutes and 4 seconds). By collecting data over a long time, one could look for a periodic signal with that period. One virtue is that systematic effects (due to daily temperature changes, for example) would more likely vary with the solar day. (Because the solar and sidereal days are so close in length, this would require a run time at least on the order of months.) One could also control for systematic effects by combining the nonparallel interferometer with a nearby standard interferometer to monitor for effects of temperature, etc. Data could be collected for long periods for different azimuthal orientations of the interferometer and different spin states. This could, at the very least, put a surprisingly stringent bound on the lattice spacing, or on other violations of Lorentz symmetry. (Of course, for a larger effect such long run times and difficult analysis would not be needed.)

One potential further complication is that the crystals making up the neutron interferometer might also display different properties in different orientations due to the discreteness of spacetime, which might also alter the relative phase shifts. It is hard to asses whether this is likely without also including a theory of electromagnetism on a discrete spacetime lattice, which we do not have at present. We see no reason to think, however, that changes in the behavior of static matter in the crystal would cancel out the changes in the moving particles passing through the interferometer, since the terms giving phase shifts are momentum dependent. Other factors—such as variable gravity effects—could also affect the strength of the signal, but seem unlikely to greatly reduce it.

C. Comparison to SME framework

Lorentz-violating terms that could be added to the Dirac equation have been parametrized within the SME framework [18,20], and experimental limits on these parameters have been found [19]. It is natural to ask whether the Lorentz-violating terms that occur in the long-wavelength expansion of the 3D quantum walk fit into this framework. Indeed, it turns out that they do. If we examine the first-order correction to the Dirac Hamiltonian in Eq. (9), we

find that it includes two sets of terms: one set that is linear in the components of momentum, and one set that is quadratic. If we adopt the Weyl representation of the Dirac spinors, we see that these give new terms in the Dirac equation of the form

$$b^{(5)XYZ}\gamma_5\gamma_X p_y p_z + b^{(5)YZX}\gamma_5\gamma_Y p_z p_x + b^{(5)ZXY}\gamma_5\gamma_Z p_x p_y + g^{XTX}\sigma_{XT}p_x + g^{YTY}\sigma_{XT}p_y + g^{ZTZ}\sigma_{XT}p_z, \tag{23}$$

where the parameters

$$b^{(5)XYZ} = -b^{(5)YZX} = b^{(5)ZXY} = c\Delta x/\hbar,$$
$$g^{XTX} = g^{YTY} = g^{ZTZ} = mc^2\Delta x/\hbar \tag{24}$$

are named according to the convention established in Ref. [20]. Experimental limits on these parameters were tabulated in Ref. [19]. These limits are derived from a wide variety of different experiments, including matter interferometry [56], atomic clock comparison tests [57], and magnetometer experiments [58]. (Many, many other experimental references are to be found in Ref. [19].)

In Ref. [19] it was described how experiments cannot necessarily put limits on the individual parameter values, but on observationally invariant linear combinations. For the g parameters above that arise from the 3D quantum walk, the relevant combinations are $\tilde{g}^{-} = m(g^{XTX} - g^{YTY})$ and $\tilde{g}^{Q} = m(g^{XTX} + g^{YTY} - 2g^{ZTZ})$. There are no experimental limits on these combinations, but in fact it does not matter, because these combinations vanish for the quantum walk system. Indeed, these terms do not contribute to the relative phase in the proposed interferometer experiment, so the experiment proposed in this paper would also not put limits on these quantities.

For the b parameters, Ref. [19] had limits on constant terms of this form, but not terms that are quadratic in momentum, like the ones that occur in Eq. (23). (In the terminology of Ref. [20], these are terms of mass dimension five rather than mass dimension three.) A more recent paper [21] has extended this analysis to put limits on terms of higher mass dimension. The tables published in that paper did not seem to include the parameters that occur in the equation derived in this paper. So the experiment proposed in this paper would extend these limits to new types of Lorentz-violating terms.

VI. CONCLUSIONS

In this paper, we employed a model of discrete spacetime based on a 3D quantum walk on the BCC lattice, which has the Dirac equation as its long-wavelength limit. Expanding the evolution operator in the small quantity $k\Delta x$, we found a perturbing Hamiltonian term that produces energy (and hence phase) shifts depending on both the direction (relative to the underlying spatial lattice) and the spin state of the particle.

Based on this Hamiltonian, we analyzed the design of a nonparallel Mach-Zehnder interferometer that would exhibit a relative phase shift between its two arms that depends on its orientation. Calculating the magnitude of this phase shift for spin-polarized thermal neutrons, we found that with current experimental accuracy, such a neutron interferometer could in principle put an upper bound on the lattice spacing Δx of 10^{-27} m to as small as 10^{-31} m—only 3 or 4 orders of magnitude away from the Planck length, and vastly smaller than the length scales probed at the LHC. It is also very possible that matter interferometers with other particles might be even more sensitive to spacetime discreteness than neutron interferometers. For example, an atom interferometer using ^{87}Rb has recently been used to probe spacetime curvature [59], and interference has been demonstrated with molecules heavier than 10^4 amu [60].

While the numbers calculated in this paper pertain only to our particular quantum walk model, there is every reason to think that other models with discrete spacetime (or other direction-dependent violations of Lorentz invariance) would behave similarly. The magnitude of the corrections is set largely by dimensional analysis; only the geometrical factors are likely to vary from model to model. It would be interesting to compare such theories, and estimate the range of effects they would produce in different interferometer configurations. It is also possible that other kinds of matter interferometry might be even better than neutrons at detecting such Lorentz-violating effects. This also seems like a question worthy of exploration.

ACKNOWLEDGMENTS

The authors acknowledge very useful information from Yuji Hasegawa, V. Alan Kostelecký, Dmitry Pushin, and Erhard Seiler, as well as interesting conversations with Chris Cantwell, Yi-Hsiang Chen, Shengshi Pang, and Chris Sutherland. They are grateful for the hospitality of Caltech's Institute for Quantum Information and Matter (IQIM).

[1] P. A. M. Dirac, Is there an Aether?, Nature (London) **168**, 906 (1951).

[2] J. D. Bjorken, A dynamical origin for the electromagnetic field, Ann. Phys. (N.Y.) **24**, 174 (1963).

[3] T. G. Pavlopoulos, Breakdown of Lorentz invariance, Phys. Rev. **159**, 1106 (1967).

[4] L. B. Rédei, Validity of special relativity at small distances and the velocity dependence of the muon lifetime, Phys. Rev. **162**, 1299 (1967).

[5] S. R. Coleman and S. L. Glashow, Cosmic ray and neutrino tests of special relativity, Phys. Lett. B **405**, 249 (1997).

[6] S. R. Coleman and S. L. Glashow, High-energy tests of Lorentz invariance, Phys. Rev. D **59**, 116008 (1999).

[7] V. A. Kostelecký and S. Samuel, Spontaneous breaking of Lorentz symmetry in string theory, Phys. Rev. D **39**, 683 (1989).

[8] J. Ellis, N. E. Mavromatos, and D. V. Nanopoulos, Probing models of quantum space-time foam, arXiv:gr-qc/9909085.

[9] C. P. Burgess, J. Cline, E. Filotas, J. Matias, and G. D. Moore, Loop-generated bounds on changes to the graviton dispersion relation, J. High Energy Phys. 03 (2002) 043.

[10] R. Gambini and J. Pullin, Nonstandard optics from quantum spacetime, Phys. Rev. D **59**, 124021 (1999).

[11] B. Carr and S. B. Giddings, Quantum black holes, Sci. Am. **292**, 48 (2007).

[12] V. A. Kostelecký and A. Mewes, Lorentz and *CPT* violation in the neutrino sector, Phys. Rev. D **70**, 031902(R) (2004).

[13] D. Mattingly, Modern tests of Lorentz invariance, Living Rev. Relativity **8**, 5 (2005).

[14] S. Liberati, Tests of Lorentz invariance: A 2013 update, Classical Quantum Gravity **30**, 133001 (2013).

[15] V. A. Kostelecky and R. Potting, *CPT*, strings, and meson factories, Phys. Rev. D **51**, 3923 (1995).

[16] D. Colladay and V. A. Kostelecky, *CPT* violation and the standard model, Phys. Rev. D **55**, 6760 (1997).

[17] D. Colladay and V. A. Kostelecky, Lorentz-violating extension of the standard model, Phys. Rev. D **58**, 116002 (1998).

[18] V. A. Kostelecky and C. D. Lane, Constraints on Lorentz violation from clock-comparison experiments, Phys. Rev. D **60**, 116010 (1999).

[19] V. A. Kostelecky and N. Russell, Data tables for Lorentz and *CPT* violation, Rev. Mod. Phys. **83**, 11 (2011); the experimental limits in this paper are regularly updated on the preprint server, arXiv:0801.0287.

[20] V. A. Kostelecky and M. Mewes, Fermions with Lorentz-violating operators of arbitrary dimension, Phys. Rev. D **88**, 096006 (2013).

[21] V. A. Kostelecky and A. J. Vargas, Lorentz and *CPT* tests with clock-comparison experiments, Phys. Rev. D **98**, 036003 (2018).

[22] Y. Aharonov, L. Davidovich, and N. Zagury, Quantum random walks, Phys. Rev. A **48**, 1687 (1993).

[23] A. Ambainis, E. Bach, A. Nayak, A. Vishwanath, and J. Watrous, *One-dimensional quantum walks, in Proceedings of the ACM Symposium on Theory of Computation (STOC01), 2001* (Association for Computing Machinery, New York, 2001), pp. 37–49.

[24] D. Aharonov, A. Ambainis, J. Kempe, and U. Vazirani, Quantum walks on graphs, in *Proceedings of the ACM Symposium on Theory of Computation (STOC01), 2001* (Association for Computing Machinery, New York, 2001), pp. 50–59.

[25] J. Kempe, Quantum walks—an introductory overview, Contemp. Phys. **44**, 307 (2003).

[26] T. A. Brun, H. A. Carteret, and A. Ambainis, The Quantum to Classical Transition for Random Walks, Phys. Rev. Lett. **91**, 130602 (2003).

[27] V. Kendon, Decoherence in quantum walks—a review, Math. Struct. Comput. Sci. **17**, 1169 (2006).

[28] I. Bialynicki-Birula, Weyl, Dirac, and Maxwell equations on a lattice as unitary cellular automata, Phys. Rev. D **49**, 6920 (1994).

[29] D. A. Meyer, From quantum cellular automata to quantum lattice gases, J. Stat. Phys. **85**, 551 (1996).

[30] F. W. Strauch, Connecting the discrete- and continuous-time quantum walks, Phys. Rev. A **74**, 030301(R) (2006).

[31] A. J. Bracken, D. Ellinas, and I. Smyrnakis, Free-Dirac-particle evolution as a quantum random walk, Phys. Rev. A **75**, 022322 (2007).

[32] C. M. Chandrashekar, S. Banerjee, and R. Srikanth, Relationship between quantum walks and relativistic quantum mechanics, Phys. Rev. A **81**, 062340 (2010).

[33] C. M. Chandrashekar, Two-state quantum walk on two- and three-dimensional lattices, arXiv:1103.2704.

[34] C. M. Chandrashekar, Two-component Dirac-like Hamiltonian for generating quantum walk on one-, two- and three-dimensional lattices, Sci. Rep. **3**, 2829 (2013).

[35] G. M. D'Ariano and P. Perinotti, Derivation of the Dirac equation from principles of information processing, Phys. Rev. A **90**, 062106 (2014).

[36] P. Arrighi, M. Forets, and V. Nesme, The Dirac equation as a quantum walk: Higher dimensions, observational convergence, J. Phys. A **47**, 465302 (2014).

[37] T. C. Farrelly and A. J. Short, Discrete spacetime and relativistic quantum particles, Phys. Rev. A **89**, 062109 (2014).

[38] G. M. D'Ariano, N. Mosco, P. Perinotti, and A. Tosini, Discrete Feynman propagator for the Weyl quantum walk in $2+1$ dimensions, Europhys. Lett. **109**, 40012 (2015).

[39] S. Succi, F. Fillion-Gourdeau, and S. Palpacelli, Quantum lattice Boltzmann is a quantum walk, EPJ Quantum Techno. **2**, 12 (2015).

[40] A. Bisio, G. M. D'Ariano, and A. Tosini, Quantum field as a quantum cellular automaton: The Dirac free evolution in one dimension, Ann. Phys. (Amsterdam) **354**, 244 (2015).

[41] P. Arrighi, S. Facchini, and M. Forets, Quantum walking in curved spacetime, arXiv:1505.07023.

[42] A. Bisio, G. M. D'Ariano, M. Erba, P. Perinotti, and A. Tosini, Quantum walks with a one-dimensional coin, Phys. Rev. A **93**, 062334 (2016).

[43] P. Arrighi and S. Facchini, Quantum walking in curved spacetime: $(3+1)$ dimensions, and beyond, arXiv:1609.00305.

[44] G. M. D'Ariano, Physics without physics: The power of information-theoretical principles, Int. J. Theor. Phys. **56**, 97 (2017).

[45] G. M. D'Ariano, M. Erba, and P. Perinotti, Isotropic quantum walks on lattices and the Weyl equation, Phys. Rev. A **96**, 062101 (2017).

[46] L. Mlodinow and T. A. Brun, Discrete spacetime, quantum walks, and relativistic wave equations, Phys. Rev. A **97**, 042131 (2018).

[47] P. Arrighi, S. Facchini, and M. Forets, Discrete Lorentz covariance for Quantum Walks and Quantum Cellular Automata, New J. Phys. **16**, 093007 (2014).

[48] A. Bisio, G. M. D'Ariano, and P. Perinotti, Quantum Walks, Weyl equation and the Lorentz group, Found. Phys. **47**, 1065 (2017).

[49] A. A. Michelson and E. W. Morley, On the relative motion of the Earth and the luminiferous ether, Am. J. Sci. **34**, 333 (1887).

[50] T. Pruttivarasin, M. Ramm, S. G. Porsev, I. I. Tupitsyn, M. S. Safronova, M. A. Hohensee, and H. Häffner, Michelson-Morley analogue for electrons using trapped ions to test Lorentz symmetry, Nature (London) **517**, 592 (2015).

[51] A. Chou *et al.*, The Holometer: An instrument to probe Planckian quantum geometry, Classical Quantum Gravity **34**, 065005 (2017).

[52] M. Zawisky, Y. Hasegawa, H. Rauch, Z. Hradil, R. Myška, and J. Peřina, Phase estimation in interferometry, J. Phys. A **31**, 551 (1998).

[53] J. Klepp, S. Sponar, and Y. Hasegawa, Fundamental phenomena of quantum mechanics explored with neutron interferometers, Prog. Theor. Exp. Phys. **2014**, 082A01 (2014).

[54] A. Cimmino, G. I. Opat, A. G. Klein, H. Kaiser, S. A. Werner, M. Arif, and R. Clothier, Observation of the Topological Aharonov-Cahser Phase Shift by Neutron Interferometry, Phys. Rev. Lett. **63**, 380 (1989).

[55] D. Sarenac, D. A. Pushin, M. G. Huber, D. S. Hussey, H. Miao, M. Arif, D. G. Cory, A. D. Cronin, B. Heacock, D. L. Jacobson, J. M. LaManna, and H. Wen, Three Phase-Grating Moire Neutron Interferometer for Large Interferometer Area Applications, Phys. Rev. Lett. **120**, 113201 (2018).

[56] H. Mueller, S.-w. Chiow, S. Herrmann, S. Chu, and K.-Y. Chung, Atom-Interferometry Tests of the Isotropy of Post-Newtonian Gravity, Phys. Rev. Lett. **100**, 031101 (2008).

[57] P. Wolf, F. Chapelet, S. Bize, and A. Clairon, Cold Atom Clock Test of Lorentz Invariance in the Matter Sector, Phys. Rev. Lett. **96**, 060801 (2006).

[58] M. Smiciklas, J. M. Brown, L. W. Cheuk, S. J. Smullin, and M. V. Romalis, New Test of Local Lorentz Invariance Using a ^{2}1Ne-Rb-K Comagnetometer, Phys. Rev. Lett. **107**, 171604 (2011).

[59] P. Asenbaum, C. Overstreet, T. Kovachy, D. D. Brown, J. M. Hogan, and M. A. Kasevich, Phase Shift in an Atom Interferometer due to Spacetime Curvature across its Wave Function, Phys. Rev. Lett. **118**, 183602 (2017).

[60] S. Eibenberger, S. Gerlich, M. Arndt, M. Mayor, and J. Tüxen, Matter-wave interference of particles selected from a molecular library with masses exceeding 10 000 amu, Phys. Chem. Chem. Phys. **15**, 14696 (2013).